THE JOURNAL OF PHYSICAL CHEMISTRY Letters

Letter

Cite This: J. Phys. Chem. Lett. 2019, 10, 4783−4787

pubs.acs.org/JPCL

Observation of the Carbon Elimination Channel in Vacuum Ultraviolet Photodissociation of OCS

Wentao Chen,[†,#] Liang Zhang,[†,#] Daofu Yuan,[†] Yao Chang,[†,‡] Shengrui Yu,[§] Siwen Wang,[†] Tao Wang,[∥] Bin Jiang,[*,†] Kaijun Yuan,[*,‡] Xueming Yang,[‡,∥] and Xingan Wang[*,†]

[†]Hefei National Laboratory for Physical Sciences at the Microscale and Department of Chemical Physics, University of Science and Technology of China, Hefei 230026, China

[‡]State Key Laboratory of Molecular Reaction Dynamics, Dalian Institute of Chemical Physics, Chinese Academy of Sciences, Dalian 116023, China

[§]Hangzhou Institute of Advanced Studies, Zhejiang Normal University, Hangzhou 311231, China

[∥]Department of Chemistry, School of Science, Southern University of Science and Technology, Shenzhen 518055, China

Supporting Information

ABSTRACT: The textbook mechanism for OCS photodissociation mainly involves the CO + S or CS + O product channel via a single bond fission. However, a third dissociation channel concerning the cleavage of both C−S and C−O bonds yielding SO + C products, though thermodynamically allowed, has never been verified experimentally to date. By using a tunable vacuum ultraviolet laser light and time-sliced velocity map ion imaging technique, we have clearly observed the $SO(X^3\Sigma^-)$ + $C(^3P_{J=0})$ products as the vacuum ultraviolet laser photon energy gradually exceeds its thermodynamic threshold. The corresponding $SO(X^3\Sigma^-)$ coproducts are highly vibrationally excited and show varying angular distributions from isotropic to anisotropic as the excitation photon energy increases. Theoretical analysis suggests that a fast nonadiabatic pathway plays a dominant role in the formation of the anisotropic SO products. That isotropic products arise as the excitation photon energies approach the thermodynamic threshold can be reasonably explained by the "roaming mechanism".

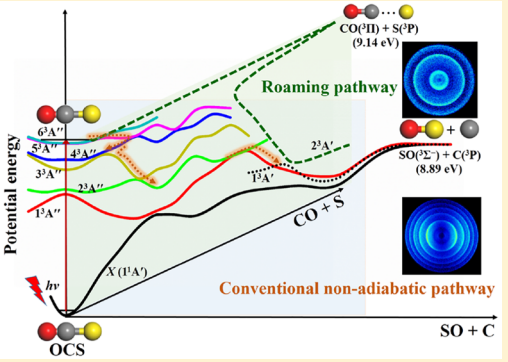

For a triatomic molecule ABC, it is well-known that the photodissociation mainly produces the AB + C and A + BC product channels via single bond fission.[1] Theoretically, however, another dissociation channel yielding AC + B products could also play a role when the excitation photon energy is sufficient. This type of dissociation has rarely been observed, and its dynamics remains unclear to date. This is because the opening of such a channel usually requires higher excitation photon energy up to the vacuum ultraviolet (VUV) region, and complicated nonadiabatic processes exist because a handful of electronically excited states are involved in the VUV region.

Carbonyl sulfide (OCS) is the most abundant sulfur-containing compound in the Earth's atmosphere. It is a climate active trace-gas,[2] a major precursor of stratospheric SO_2, and plays a very important role in atmospheric chemistry.[3−6] The photodissociation of OCS is a significant sink channel and produces various radicals; therefore, OCS has long been a benchmark system in understanding photodissociation dynamics of small molecules.[7,8] Over the past two decades or so, photodissociation of OCS has been extensively investigated particularly for the $CO(^1\Sigma^+)$ + $S(^1D)$ channel in the UV region, both experimentally[9−14] and theoretically,[15−19] with a special focus on the polarization of atomic fragments and the photolysis of oriented molecules.[20−24]

As the photon energy increases up to the VUV region, the following channels become energetically accessible:

$$OCS + h\nu \rightarrow CO(^1\Sigma^+) + S(^1S) \quad (1)$$

$$\rightarrow CS(^1\Sigma^+) + O(^3P/^1D) \quad (2)$$

$$\rightarrow SO(^3\Sigma^-) + C(^3P) \quad (3)$$

The single bond fission channels 1 and 2 have also been experimentally observed[25] in the VUV region[26−28] and have been well-documented as textbook examples. However, channel 3, which requires both the C−S and C−O bonds to be broken and a new S−O bond to be formed, is a very interesting process and has never been verified experimentally. To the best of our knowledge, the only example of such a central-atom elimination process for triatomic molecules is the O_2 production in the photodissociation of CO_2, which was

Received: June 23, 2019
Accepted: August 4, 2019
Published: August 5, 2019

DOI: 10.1021/acs.jpclett.9b01811
J. Phys. Chem. Lett. 2019, 10, 4783−4787

reported by Ng and co-workers very recently at the photolysis wavelengths between 101.5 and 107.2 nm.[29] However, because of the limited experimental resolution and the lack of detailed theoretical analysis, the underlying mechanism for this new type of photodissociation channel remains unclear.

Here we report a synergistic experimental and theoretical study on VUV photodissociation of OCS→ $SO(^3\Sigma^-)$ + $C(^3P)$. The experiments were carried out using a time-sliced velocity map ion imaging (VMI) setup with very high energy and angular resolutions, which has been described previously[30−33] and in the Supporting Information. By detecting the ion images of $C(^3P_{J=0})$ products, the SO + C channel was clearly observed. Furthermore, a remarkable variation has been observed in the product angular distribution as a function of photolysis wavelength. Ab initio calculations have revealed two possible mechanisms depending on the excitation energy, offering a reasonable interpretation to experimental findings.

As shown on the left of Figure 1, the time-sliced ion images of the $C(^3P_{J=0})$ products were recorded at six VUV photolysis wavelengths, i.e., 138.53, 135.84, 134.57, 129.32, 128.14, and 126.08 nm, which correspond to the excitations of the parent OCS molecule to a series of vibrational states in the F and P Rydberg states.[34] At all six photolysis wavelengths, well-resolved concentric rings with different intensities are clearly observed in the experimental images, which can be directly attributed to different vibrational states of the $SO(X^3\Sigma^-)$ coproducts. It is noted that these structures cannot arise from the other C elimination process, i.e., the C + S + O channel, because of the insufficient photolysis photon energy. The two-photon process is not possible because of the extremely low intensity of the VUV light.

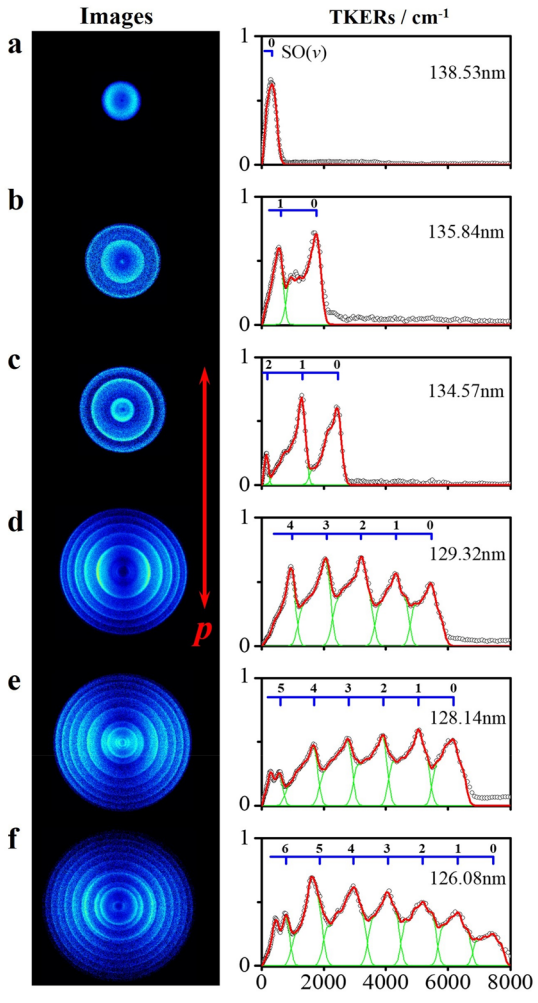

Figure 1. Ion images and TKER distributions (arb. units) of $C(^3P_{J=0})$ products from the photodissociation of OCS at wavelengths (a) 138.53 nm, (b) 135.84 nm, (c) 134.57 nm, (d) 129.32 nm, (e) 128.14 nm, and (f) 126.08 nm. The rings shown in the images correspond to the vibrational state of the $SO(X^3\Sigma^-)$ coproducts.

The velocity distributions of the $C(^3P_{J=0})$ products were obtained by integrating the signal at a specific velocity over all product angles, from which the total kinetic energy release (TKER) distributions are derived and shown on the right of Figure 1. According to the law of energy conservation (see the Supporting Information), the maximum product kinetic energy can be used to deduce the threshold energy D_0 (≈8.89 eV) (see the Supporting Information). The photon energy of the longest photolysis wavelength, i.e., 138.53 nm (~8.94 eV), is right above the dissociation threshold of the $SO(X^3\Sigma^-)$ + $C(^3P)$ channel. This suggests that the carbon elimination channel bears no or a quite small kinetic barrier. The internal energy distributions of $SO(X^3\Sigma^-)$ coproducts can be obtained from the TKER spectra by using the law of energy conservation. The energy combs representing the vibrational quantum numbers v of $SO(X^3\Sigma^-)$ products are labeled in Figure 1. The $SO(X^3\Sigma^-)$ products show very high vibrational excitation with modest rotational excitation.

The angular distributions corresponding to each $SO(X^3\Sigma^-)$ vibrational state could be extracted from the images by integrating the intensity over the corresponding radial range for each vibrational peak. The results were fitted by the following equation:

$$I(\theta) = (1/4\pi)[1 + \beta P_2(\cos\theta)] \quad (4)$$

where $P_2(x)$ is the second-order Legendre polynomial and θ is the crossing angle between the recoil velocity of the atomic carbon products and the polarization of the VUV photolysis laser. The angular anisotropy value β ranges from −1 to 2, providing information about the photodissociation rates (faster or slower than the rotational period of the excited OCS molecules) for the formation of specific products, as well as the symmetry of the excited states. The vibrational state-resolved β values at the six photolysis wavelengths are derived and shown in Figure 2. At each wavelength, the β values show very weak dependence on the vibrational excitation of the $SO(X^3\Sigma^-)$ products, suggesting that the $SO(X^3\Sigma^-)$ products with different vibrational excitations may follow a similar dissoci-

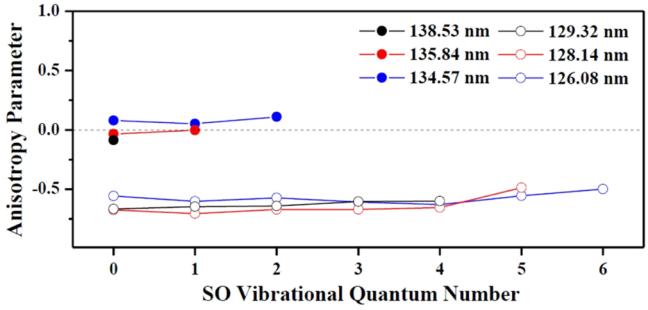

Figure 2. Anisotropy parameters (β values) for individual vibrational states of $SO(X^3\Sigma^-)$ product at six different photolysis wavelengths between 138.53 and 126.08 nm.

DOI: 10.1021/acs.jpclett.9b01811
J. Phys. Chem. Lett. 2019, 10, 4783−4787

ation mechanism at a given excitation energy. Furthermore, two distinctly different angular distributions are observed. At the three short wavelengths, 129.32, 128.14, and 126.08 nm, the angular distributions are obviously anisotropic, with β values around −0.5 to −0.7, suggesting that the dissociation must be fast. At the three longer photolysis wavelengths, the SO($X^3\Sigma^-$) products show nearly isotropic angular distribution with β values being very close to 0, indicating that this dissociation process should be quite slow.

To characterize the dissociation mechanisms of OCS photolysis via these high-lying states, we have explored the potential energy curves of electronic states up to ∼10 eV for the first time, by means of high-level internally contracted multireference configuration interaction (ic-MRCI) calculations[35,36] (see the Supporting Information for more details). These high-lying states, many of which were absent in previous theoretical studies,[16] possess mixed valence−Rydberg character that are dominated by the electronic transitions from the highest occupied molecular orbital 3π to the unoccupied molecular/Rydberg orbitals. At the experimental photoexcitation energies, the OCS molecule is likely to populate on the vibrational bands of F $3^1\Pi$ and P $2^3\Sigma^-$ states, as analyzed in the Supporting Information and shown in Figure S2. Schinke and co-workers have shown that spin-forbidden transitions of OCS from X $1^1\Sigma^+$ to c $1^3\Sigma^-$ state can take place via strong spin−orbit couplings,[16] and we also found here sufficiently large spin−orbit-induced transition dipole moment from X $1^1\Sigma^+$ to P $2^3\Sigma^-$ states supporting the electronic transitions to this state (see the Supporting Information).

Ng and co-workers[29] recently reported the formation of the O_2 + C products via the VUV photodissociation of CO_2. They speculated a possible pathway where the excited CO_2 molecule goes through internal conversion to the ground state, followed by formation of the cyclic CO_2 complex and a collinear COO intermediate before dissociating to $O_2(^3\Sigma_g^-)$ + C(^{3}P). A detailed theoretical analysis was not given in that work, although some avoided crossings among relevant excited states have been seen theoretically.[37]

Because OCS is an asymmetric molecule, we identify several local minima on the ground state of OCS, whose energies and geometries are given in Figure S4. In Figure 3, we have drawn out a possible pathway from the Franck−Condon point to the SO + C products via two bent local minima (LM1 and LM2), representing the rotation of the O atom from one side to the other, as a function of the linearly interpolated internal coordinate. The density of electronic states close to 9 eV is extremely high (see Figure S5). These states feature shallow wells near the Franck−Condon region, which support numerous superimposed vibrational states bearing strong vibronic and/or spin−orbit couplings. In Figure 3, for example, the molecule excited to the $6^3A''$ (P $2^3\Sigma^-$ at linearity) state may undergo a series of internal conversions (marked by arrows) via avoided crossings between adjacent states, quickly relaxing to the $2^3A''$ state before reaching LM1. Nonadiabatic transition can further occur between $2^3A''$ and $1^3A''$ states near the strong coupling region between LM1 and LM2, after which the molecule would be able to dissociate adiabatically to the SO($X^3\Sigma^-$) + C(^{3}P) products.

It should be emphasized that the realistic nonadiabatic pathways could be much more complicated and span over the three-dimensional configuration space, which cannot be quantitatively determined without explicit quantum/classical dynamics calculations with these high-lying coupled PESs that

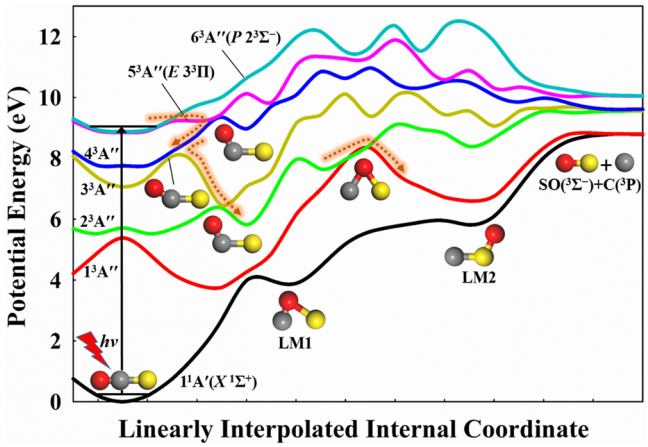

Figure 3. Potential energy curves of the ground singlet state and the lowest 6 triplet states in A″ symmetry along the linearly interpolated internal coordinate from the linear OCS equilibrium to SO + C products via two bent local minima (LM1 and LM2). The dashed arrows indicate a possible nonadiabatic pathway for photodissociation of OCS to this channel.

are beyond the current level of theory. However, it is interesting to note that those nonadiabatic transitions mainly occur at those geometries with an elongated S−O bond length compared that of the isolated SO molecule. This means that the S−O bond is not yet formed when the C−S bond starts to dissociate. The extra potential energy is expected to deposit in the S−O vibration, leading to very hot vibrational distributions of the SO product. In addition, the anisotropic angular distribution indicates that the dissociation process must occur relatively fast, consistent with the strong nonadiabatic couplings. The experimentally observed SO(X) products with large anisotropic angular β values (−0.5 to −0.7) at wavelengths shorter than 130 nm suggest that the above dissociation pathway may dominate the OCS photodissociation in this excitation energy range.

In contrast, the product angular distributions obtained from photodissociation at 138.53, 135.84, and 134.5 nm are almost isotropic, which seem to indicate a different dissociation pathway that occurs more slowly. Recent experimental and theoretical studies have identified a "roaming" mechanism in photodissociation of polyatomic molecules, whose dynamical signature includes the highly vibrationally excited and isotropically distributed products.[38−40] The excited state roaming pathway is also possible for OCS photodissociation, similar to that observed in NO_3 photodissociation.[40] As seen in Figure S6, we show that various CO + S channels are actually accessible in our experiment. Interestingly, the OCS molecule excited at these three long wavelengths is energetically quite close to the CO($^3\Pi$) + S(^{3}P) dissociation limit (∼9.14 eV). In such cases, a molecule attempting to access this product channel could have insufficient energy to dissociate. The sulfur atom can be gradually pulled back by the long-range interaction between the CO + S fragments, followed by a long time of roaming and relaxation to the lower states, with the final intramolecular abstraction of the oxygen by the sulfur atom from the CO fragment. A schematic diagram for such a pathway is given in Figure 4 via the a ($1^3A'$) state. In this dissociation process, the SO product is also highly vibrationally excited because of bond stretching in the sudden intramolecular abstraction process, which is hardly distinguishable

DOI: 10.1021/acs.jpclett.9b01811
J. Phys. Chem. Lett. 2019, 10, 4783−4787

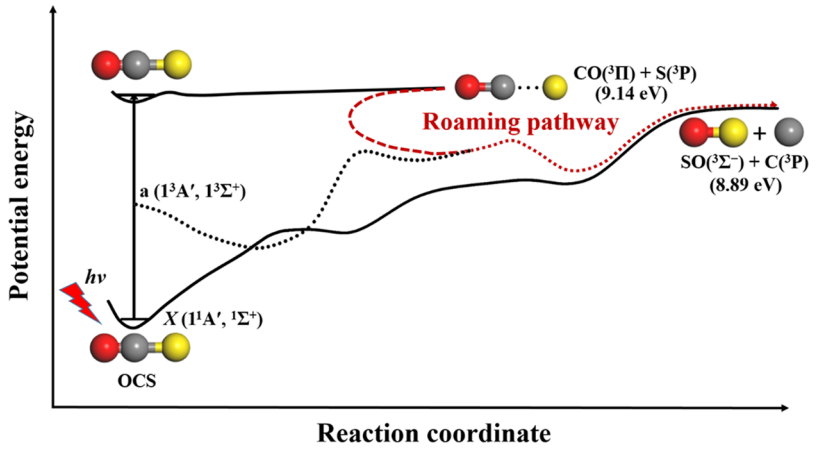

Figure 4. Schematic potential energy diagram for the representative roaming pathway going through the $1^3A'$ state to the SO + C products. Product energies are estimated from thermodynamic data.

from that generated via the conventional nonadiabatic dissociation pathway. Fortunately, the dissociation process via the roaming mechanism is quite slow, leading to isotropic angular distribution. This is exactly what we have observed in experiments of OCS photodissociation at longer excitation wavelengths. Combined parallel and perpendicular transitions can also lead to an isotopic angular distribution. This however requires at least two electronic states with different symmetry (the parallel and perpendicular transitions should be reached to excited states with different symmetry) being excited with similar transition possibilities, and the two states have similar coupling strengths with lower electronic states, which seems unlikely to happen at a set of photolysis wavelengths.

Ng and co-workers[29] have also speculated a roaming mechanism in their CO_2 photodissociation experiment. However, the anisotropic angular distributions in that work offer less unambiguous evidence for the roaming pathway. By contrast, in our case, we propose that the roaming mechanism may dominate at the excitation energies near the threshold of the $CO(^3\Pi) + S(^3P)$ dissociation channel, as seen in Figure 4. It becomes however less important at short excitation wavelengths (i.e., 129.32, 128.14, and 126.08 nm) via the P state, because the molecule now has enough energy to enable facile dissociation to the $CO(^3\Pi) + S(^3P)$ products. The conventional nonadiabatic pathways thus become the primary mechanism for $SO(X^3\Sigma^-) + C(^3P)$ product formation at higher photolysis photon energies.

To summarize, we have investigated the photodissociation dynamics of OCS + $h\nu \rightarrow SO(X^3\Sigma^-) + C(^3P)$ in a combined experimental and theoretical study. The product state and angular distributions of $SO(X^3\Sigma^-)$ produced at six VUV wavelengths show clear evidence of two distinct dissociation pathways. High-level multistate ab initio calculations suggest two possible mechanisms. One is a conventional nonadiabatic pathway dominating at higher excitation energies, in which the molecules follow a series of fast internal conversions from the initial excited state to lower electronic states and then dissociate on these low-lying states. The other is a roaming pathway that may be dominant near the energy threshold of the $CO(^3\Pi) + S(^3P)$ channel, which well explains the nearly isotropic angular distribution in this energy range. Given the demonstrations of OCS and CO_2, we believe that this central-atom elimination channel may be more general than expected in the photodissociation of triatomic molecules.

■ ASSOCIATED CONTENT

Supporting Information

The Supporting Information is available free of charge on the ACS Publications website at DOI: 10.1021/acs.jpclett.9b01811.

Experimental methods and computational details (PDF)

■ AUTHOR INFORMATION

Corresponding Authors

*E-mail: bjiangch@ustc.edu.cn (B.J.).
*E-mail: kjyuan@dicp.ac.cn (K.Y.).
*E-mail: xawang@ustc.edu.cn (X.W.).

ORCID

Tao Wang: 0000-0002-6091-1020
Bin Jiang: 0000-0003-2696-5436
Kaijun Yuan: 0000-0002-5108-8984
Xingan Wang: 0000-0002-1206-7021

Author Contributions

#W.C. and L.Z. contributed equally in this work.

Notes

The authors declare no competing financial interest.

■ ACKNOWLEDGMENTS

This work was supported by the National Key R&D Program of China, (Grant Nos. 2016YFF0200500 and 2017YFA0303500), the National Natural Science Foundation of China (Grant Nos. 21473173, 21590802, 21773213, 21722306, and 21673232), the Strategic Priority Research Program of Chinese Academy of Sciences (Grant No. XDB17000000), the Fundamental Research Funds for the Central Universities, and Anhui Initiative in Quantum Information Technologies.

■ REFERENCES

(1) Okabe, H. *Photochemistry of Small Molecules*; Wiley: New York, 1978.

(2) Lennartz, S. T.; Marandino, C. A.; von Hobe, M.; Cortes, P.; Quack, B.; Simo, R.; Booge, D.; Pozzer, A.; Steinhoff, T.; Arevalo-Martinez, D. L.; Kloss, C.; Bracher, A.; Röttgers, R.; Atlas, E.; Krüger, K. Direct Oceanic Emissions Unlikely to Account for the Missing Source of Atmospheric Carbonyl Sulfide. *Atmos. Chem. Phys.* **2017**, *17*, 385−402.

DOI: 10.1021/acs.jpclett.9b01811
J. Phys. Chem. Lett. 2019, 10, 4783−4787

(3) Pham, M.; Mueller, J.-F.; Brasseur, G. P.; Granier, C.; Mégie, G. A Three-Dimensional Study of the Tropospheric Sulfur Cycle. *J. Geophys. Res.* **1995**, *100*, 26061−26092.
(4) Montzka, S. A.; Calvert, P.; Hall, B. D.; Elkins, J. W.; Conway, T. J.; Tans, P. P.; Sweeney, C. On the Global Distribution, Seasonality, and Budget of Atmospheric Carbonyl Sulfide (COS) and some Similarities to CO_2. *J. Geophys. Res.* **2007**, *112*, D09302.
(5) Kjellstrom, E. A Three-Dimensional Global Model Study of Carbonyl Sulfide in the Troposphere and the Lower Stratosphere. *J. Atmos. Chem.* **1998**, *29*, 151−177.
(6) Thornton, D. C.; Bandy, A. R.; Blomquist, B. W.; Anderson, B. E. Impact of Anthropogenic and Biogenic Sources and Sinks on Carbonyl Sulfide in the North Pacific Troposphere. *J. Geophys. Res.* **1996**, *101*, 1873−1881.
(7) Schinke, R. *Photodissociation Dynamics: Spectroscopy and Fragmentation of Small Polyatomic Molecules*; Cambridge University Press: Cambridge, U.K., 1995.
(8) Brouard, M.; Quadrini, F.; Vallance, C. The Photodissociation Dynamics of OCS at 248 nm: The S (^3P_J) Atomic Angular Momentum Polarization. *J. Chem. Phys.* **2007**, *127*, No. 084305.
(9) Katayanagi, H.; Mo, Y. X.; Suzuki, T. 223nm Photodissociation of OCS: Two Components in S($^1D_2$) and S($^3P_2$) Channels. *Chem. Phys. Lett.* **1995**, *247*, 571−576.
(10) Sato, Y.; Matsumi, Y.; Kawasaki, M.; Tsukiyama, K.; Bersohn, R. Ion Imaging of the Photodissociation of OCS near 217 and 230 nm. *J. Phys. Chem.* **1995**, *99*, 16307−16314.
(11) Suzuki, T.; Katayanagi, H.; Nanbu, S.; Aoyagi, M. Nonadiabatic Bending Dissociation in 16 Valence Electron System OCS. *J. Chem. Phys.* **1998**, *109*, 5778−5794.
(12) Katayanagi, H.; Suzuki, T. Non-Adiabatic Bending Dissociation of OCS: the Effect of Bending Excitation on the Transition Probability. *Chem. Phys. Lett.* **2002**, *360*, 104−110.
(13) van den Brom, A. J.; Rakitzis, T. P.; van Heyst, J.; Kitsopoulos, T. N.; Jezowski, S. R.; Janssen, M. H. M. State-to-State Photodissociation of OCS(v_2=0,1|*JIM*). I. The Angular Recoil Distribution of CO ($X^1\Sigma^+$; v = 0|J). *J. Chem. Phys.* **2002**, *117*, 4255−4263.
(14) Laura Lipciuc, M.; Janssen, M. H. M. Slice Imaging of Quantum State-to-State Photodissociation Dynamics of OCS. *Phys. Chem. Chem. Phys.* **2006**, *8*, 3007−3016.
(15) Schmidt, J. A.; Johnson, M. S.; McBane, G. C.; Schinke, R. Communication: Multi-State Analysis of the OCS Ultraviolet Absorption Including Vibrational Structure. *J. Chem. Phys.* **2012**, *136*, 131101.
(16) Schmidt, J. A.; Johnson, M. S.; McBane, G. C.; Schinke, R. The Ultraviolet Spectrum of OCS from First Principles: Electronic Transitions, Vibrational Structure and Temperature Dependence. *J. Chem. Phys.* **2012**, *137*, No. 054313.
(17) McBane, G. C.; Schmidt, J. A.; Johnson, M. S.; Schinke, R. Ultraviolet Photodissociation of OCS: Product Energy and Angular Distributions. *J. Chem. Phys.* **2013**, *138*, No. 094314.
(18) Schmidt, J. A.; Olsen, J. M. H. Photodissociation of OCS: Deviations between Theory and Experiment, and the Importance of Higher Order Correlation Effects. *J. Chem. Phys.* **2014**, *141*, 184310.
(19) Schmidt, J. A.; Johnson, M. S.; Hattori, S.; Yoshida, N.; Nanbu, S.; Schinke, R. OCS Photolytic Isotope Effects from First Principles: Sulfur and Carbon Isotopes, Temperature Dependence and Implications for the Stratosphere. *Atmos. Chem. Phys.* **2013**, *13*, 1511−1520.
(20) Kim, Z. H.; Alexander, A. J.; Zare, R. N. Speed-Dependent Photofragment Orientation in the Photodissociation of OCS at 223 nm. *J. Phys. Chem. A* **1999**, *103*, 10144−10148.
(21) Lee, S. K.; Silva, R.; Thamanna, S.; Vasyutinskii, O. S.; Suits, A. G. S($^1D_2$) Atomic Orbital Polarization in the Photodissociation of OCS at 193 nm: Construction of the Complete Density Matrix. *J. Chem. Phys.* **2006**, *125*, 144318.
(22) Brouard, M.; Green, A. V.; Quadrini, F.; Vallance, C. Photodissociation Dynamics of OCS at 248 nm: The S($^1D_2$) Atomic Angular Momentum Polarization. *J. Chem. Phys.* **2007**, *127*, No. 084304.
(23) Rakitzis, T. P.; van den Brom, A.; Janssen, M. H. M. Directional Dynamics in the Photodissociation of Oriented Molecules. *Science* **2004**, *303*, 1852−1854.
(24) Sofikitis, D.; Suarez, J.; Schmidt, J. A.; Rakitzis, T. P.; Farantos, S. C.; Janssen, M. H. M. Recoil Inversion in the Photodissociation of Carbonyl Sulfide near 234nm. *Phys. Rev. Lett.* **2017**, *118*, 253001.
(25) Sugita, A.; Mashino, M.; Kawasaki, M.; Matsumi, Y.; Bersohn, R.; Trott-Kriegeskorte, G.; Gericke, K. H. Effect of Molecular Bending on the Photodissociation of OCS. *J. Chem. Phys.* **2000**, *112*, 7095−7101.
(26) Wu, S. M.; Yang, X.; Parker, D. H. Velocity Map Imaging Study of OCS Photodissociation Followed by S(^1S) Autoionization at 157 nm. *Mol. Phys.* **2005**, *103*, 1797−1807.
(27) Yamanouchi, K.; Ohde, K.; Hishikawa, A.; Pibel, C. D. Photodissociation and Vibrational Dynamics of OCS in the VUV Region. *Bull. Chem. Soc. Jpn.* **1995**, *68*, 2459−2464.
(28) Itakura, R.; Hishikawa, A.; Yamanouchi, K. Resonance-State Selective Photodissociation of OCS (2 $^1\Sigma^+$): Rotational and Vibrational Distributions of CO Fragments. *J. Chem. Phys.* **2000**, *113*, 6598−6607.
(29) Lu, Z.; Chang, Y. C.; Yin, Q. Z.; Ng, C. Y.; Jackson, W. M. Evidence for Direct Molecular Oxygen Production in CO_2 Photodissociation. *Science* **2014**, *346*, 61−64.
(30) Yu, S. R.; Yuan, D. F.; Chen, W. T.; Yang, X. M.; Wang, X. A. VUV Photodissociation Dynamics of Nitrous Oxide: The O($^1S_{J=0}$) and O($^3P_{J=2,1,0}$) Product Channels. *J. Phys. Chem. A* **2015**, *119*, 8090−8096.
(31) Yuan, D. F.; Yu, S. R.; Cheng, W.; Xie, T.; Yang, X. M.; Wang, X. A. VUV Photodissociation Dynamics of Nitrous Oxide: The N($^2D_{J=3/2,5/2}$) and N($^2P_{J=1/2,3/2}$) Product Channels. *J. Phys. Chem. A* **2016**, *120*, 4966−4972.
(32) Yuan, D. F.; Yu, S. R.; Xie, T.; Chen, W. T.; Wang, S. W.; Tan, Y. X.; Wang, T.; Yuan, K. J.; Yang, X. M.; Wang, X. A. Photodissociation Dynamics of Nitrous Oxide near 145 nm: The O($^1S_0$) and O($^3P_{J=2,1,0}$) Product Channels. *J. Phys. Chem. A* **2018**, *122*, 2663−2669.
(33) Yu, S. R.; Yuana, D. F.; Chen, W. T.; Xie, T.; Wang, S. W.; Yang, X. M.; Wang, X. A. High-Resolution Experimental Study on Photodissociation of N_2O. *Chin. J. Chem. Phys.* **2016**, *29*, 135−139.
(34) Limao-Vieira, P.; Ferreira da Silva, F.; Almeida, D.; Hoshino, M.; Tanaka, H.; Mogi, D.; Tanioka, T.; Mason, N. J.; Hoffmann, S. V.; Hubin-Franskin, M. J.; Delwiche, J. Electronic Excitation of Carbonyl Sulphide (COS) by High-Resolution Vacuum Ultraviolet Photoabsorption and Electron-Impact Spectroscopy in the Energy Region from 4 to 11 eV. *J. Chem. Phys.* **2015**, *142*, No. 064303.
(35) Knowles, P. J.; Werner, H.-J. An Efficient Method for the Evaluation of Coupling Coefficients in Configuration Interaction Calculations. *Chem. Phys. Lett.* **1988**, *145*, 514−522.
(36) Werner, H.-J.; Knowles, P. J. An Efficient Internally Contracted Multiconfiguration-Reference Configuration Interaction Method. *J. Chem. Phys.* **1988**, *89*, 5803−5814.
(37) Grebenshchikov, S. Y. Photodissociation of Carbon Dioxide in Singlet Valence Electronic States. I. Six Multiply Intersecting Ab Initio Potential Energy Surfaces. *J. Chem. Phys.* **2013**, *138*, 224106.
(38) Townsend, D.; Lahankar, S. A.; Lee, S. K.; Chambreau, S. D.; Suits, A. G.; Zhang, X.; Rheinecker, J.; Harding, L. B.; Bowman, J. M. The Roaming Atom: Straying from the Reaction Path in Formaldehyde Decomposition. *Science* **2004**, *306*, 1158−1161.
(39) Suits, A. G. Roaming Atoms and Radicals: A New Mechanism in Molecular Dissociation. *Acc. Chem. Res.* **2008**, *41*, 873−881.
(40) Grubb, M. P.; Warter, M. L.; Xiao, H.; Maeda, S.; Morokuma, K.; North, S. W. No Straight Path: Roaming in the Both Ground- and Excited-State Photolytic Channels of $NO_3 \rightarrow NO + O_2$. *Science* **2012**, *335*, 1075−1078.

DOI: 10.1021/acs.jpclett.9b01811
J. Phys. Chem. Lett. 2019, 10, 4783−4787